

NEUTRON STARS: FORMATION AND STRUCTURE^{*)}

Marek Kutschera

H. Niewodniczański Institute of Nuclear Physics
ul. Radzikowskiego 152, 31-342 Kraków, Poland

and

Institute of Physics, Jagellonian University
ul. Reymonta 4, 30-059 Kraków, Poland

Abstract:

A short introduction is given to astrophysics of neutron stars and to physics of dense matter in neutron stars. Observed properties of astrophysical objects containing neutron stars are discussed. Current scenarios regarding formation and evolution of neutron stars in those objects are presented. Physical principles governing the internal structure of neutron stars are considered with special emphasis on the possible spin ordering in the neutron star matter.

PACS: 21.65.+f,97.60.Jd

1. INTRODUCTION

The existence of compact stars stabilized by the neutron pressure was predicted soon after discovery of the neutron [1]. The idea of neutron stars is thus more than 60 years old. The first observation was made only 30 years later in 1967. The history of the idea and of actual discovery of neutron stars can be found in Ref.[1].

The first radio pulsar was discovered by Bell and Hewish in November 1967 [1]. Soon after the discovery radio pulsars were identified with rotating magnetized neutron stars [1]. Since then a number of astrophysical objects involving neutron stars have been observed both in radio and X-ray bands. These include millisecond pulsars, binary radio pulsars,

^{*)} Lectures given at the XXV Mazurian Lakes School of Physics, Piaski, August 1997.

high-mass X-ray binaries and low-mass X-ray binaries. Recently, an isolated nonpulsating neutron star which radiates thermally was observed by the Hubble Space Telescope [2]. The star is less than 130 pc from Earth.

The aim of these lectures is to give an introduction to both astrophysics of neutron stars and physics of neutron star structure. In Sect.2 a brief review of the astrophysical objects which contain neutron stars is given. I will shortly describe observed properties of these objects. In Sect.3 current scenarios of formation of neutron stars in these objects are presented. In Sect.4 I will outline some basic ideas regarding the neutron star structure. An emphasis will be given to the behaviour of proton component of the neutron star matter. In particular, a possible spin ordering in the neutron star core and its implications for neutron stars are discussed.

2. ASTROPHYSICS OF NEUTRON STARS

Astrophysical objects in hydrostatic equilibrium fall in four different categories according to the physical nature of pressure which supports them against gravity. The source of pressure in normal stars and in white dwarfs is the kinetic energy of, respectively, a thermal plasma and a degenerate electron gas. In planets and neutron stars the pressure is due to the interaction energy of, respectively, a condensed atomic matter and a condensed nucleon (hadronic) matter.

Here we are interested mostly in neutron stars. From the fact that hadronic pressure becomes relevant only at a sufficiently high density when the nucleons start to feel their mutual repulsion we can infer the density and the size of neutron stars. The repulsive core of nucleon-nucleon interactions start to dominate at densities exceeding the saturation density of nuclear matter, $n > n_0 = 0.17 fm^{-3}$ (or mass density $\rho > \rho_0 = n_0(m_P - B/c^2) \approx 2.7 \times 10^{14} g/cm^3$). The radius of a $1M_\odot$ star of density ρ_0 is $R \approx 12km$. Hence neutron stars, objects stabilized by the nucleon (hadron) pressure, have densities of the order of nuclear matter density and radii of the order of $10km$.

Neutron stars, discovered initially as radio pulsars, are responsible for a number of astrophysical phenomena. Below we discuss in some detail astrophysical objects containing neutron stars.

2.1. Radio pulsars

Radio pulsars are rapidly rotating strongly magnetized neutron stars. Their rotation period, P , is in the range $0.033s \leq P \leq 4.0s$. Pulsars emit radiation at the expense of

the rotational energy. As a result, they spin down. The spin-down rate \dot{P} is measured to be $\sim 10^{-12} - 10^{-16} \text{ss}^{-1}$. Measurements of the period, P , and its derivative, \dot{P} , allow us to obtain the magnetic field of the pulsar, B , assuming that the spin-down is due to the dipole magnetic braking. A simple formula for the pulsar "luminosity" is

$$L_{pulsar} = \frac{2R^6}{3c^3} \left(\frac{2\pi}{P}\right)^4 B^2 = -\dot{E}_{rot}, \quad (1)$$

where the pulsar rotational energy is $E_{rot} = I(2\pi/P)^2/2$. From Eq.(1) we find that the magnetic field is $B = 3.2 \times 10^{19} \sqrt{P\dot{P}}$, with P in seconds. In this estimate, typical values of the moment of inertia, $I = 10^{45} \text{gcm}^2$, and the radius, $R = 10 \text{km}$, are used. Pulsar magnetic fields are found to be $B \sim 10^{11} - 10^{13} \text{G}$.

The total radio luminosity of pulsars is generally $\sim 10^{26} - 10^{30} \text{erg/s}$. These values are some two to six orders of magnitude below the rate \dot{E}_{rot} of rotational energy dissipation. Pulsars obviously emit energy at other wavelengths.

One of the best studied pulsars is the Crab pulsar, PSR 0531+21, with the period $P = 0.033 \text{s}$. The neutron star (Crab pulsar) and the Crab nebula in which the pulsar is embedded are remnants of the supernova in the year 1054. The Crab pulsar is thus about 940 years old. It is the youngest known pulsar. The Crab pulsar is observed optically as a faint star near the center of the Crab nebula. The pulsar radiates also in X- and γ -rays. In all bands, at radio frequencies, in visible light, in X-rays and in γ -rays the signal displays the same pulse profile, Fig.1. According to current theories of pulsar emission, the pulsating radiation at all wavelengths is produced by the same magnetospheric activity which generates the radio signal. This means that the visible light is not emitted from the surface of the neutron star but rather from an extended magnetosphere. Optical observations of the Crab pulsar do not allow us to constrain the radius of the star.

2.1.1. Millisecond pulsars

There exists a clearly distinct category of radio pulsars, millisecond pulsars, with short periods in the range $1.56 \text{ms} \leq P \leq 100 \text{ms}$ and very small period derivatives, $\dot{P} \sim 10^{-17} - 10^{-21}$. The fact that corresponding magnetic fields are much weaker than for ordinary pulsars, $B \sim 10^8 - 10^{10} \text{G}$, strongly suggests that millisecond pulsars should be treated as a different class of radio pulsars. Almost one half of all millisecond pulsars are members of binary systems, which is another distinct feature of these objects. The fastest known pulsar, PSR 1937+21, has the period $P = 1.56 \text{ms}$ and $\dot{P} = 10^{-19}$. Some

researchers [3] postulate that millisecond pulsars with lowest magnetic fields, $B \sim 10^8 G$, are of different origin than those with higher fields.

2.2. X-ray binaries

X-ray observations made by satellite experiments have revealed the existence of binary systems composed of the neutron star with the companion which is a normal star. There are two classes of such binary stars, high mass X-ray binaries and low mass X-ray binaries. In both cases, the neutron star is accreting matter from the companion, which results in X-ray emission. However the pattern of the X-ray emission is different for both classes.

2.2.1. High mass X-ray binaries

The X-ray flux of high-mass X-ray binaries displays a periodic modulation, hence these objects are also called X-ray pulsars. The companion of the neutron star is usually a massive O or B star with the mass $\sim 10M_\odot - 40M_\odot$. The neutron star is strongly magnetized with the magnetic field typical for normal radio pulsars, $B \sim 10^{12} - 10^{13} G$. Matter accreted onto the neutron star moves along the magnetic field lines and hits the neutron star surface in the vicinity of the magnetic pole. In this way, a hot spot emitting X-rays is formed around the magnetic pole. Rotation of the neutron star around an axis inclined with respect to the magnetic axis produces the pulsar effect. The rotation period of X-ray pulsars ranges from $P \sim 0.1s$ to a fraction of an hour. The slowest X-ray pulsar has the period $P \sim 1400s$ [4]. Since heavy stars live short the age of high mass X-ray binaries is estimated to be less than $10^7 y$. Recent review of X-ray pulsars is given in Ref.[5].

One should note that for some accreting X-ray pulsars the rotation period decreases, $\dot{P} < 0$. Apparently, these pulsars are spinning up due to accretion of matter.

2.2.2. Low mass X-ray binaries

The companion of the neutron star in low mass X-ray binaries is a faint star with the mass $M \leq 1.2M_\odot$. The X-ray emission displays bursts which repeat in several hours. Low mass X-ray binaries are also named X-ray bursters. The X-ray bursts are thought to be produced by a thermonuclear flash of the accreted nuclear fuel. Accreted matter spreads over the surface of the neutron star. This occurs because the magnetic field is low, $B \leq 10^{10} G$. Continuous accretion from the companion increases the density and temperature at the base of the fuel shell. When the condition of instability is reached, a

nuclear flash occurs. A new shell of fuel is then accreted and the cycle repeats. The X-ray busters are rather old objects, with the age more than 10^8 years.

2.3. Binary radio pulsars

An important class of neutron star binaries are systems where the neutron star is detected as a radio pulsar. Such systems are binaries with no mass transfer. The best studied binary radio pulsar is the Hulse and Taylor pulsar, PSR 1913+16 [6]. Generally, one can distinguish two subclasses of these objects, close systems with a compact companion, PSR 1913+16 subclass, and loose systems with the companion being low-mass faint star, PSR 1953+29 subclass. In the former case the orbit is tight and eccentric with the orbital period $P_{orb} \sim 1day$. The compact companion is a neutron star or a massive white dwarf ($M \approx 1.4M_{\odot}$). In the latter case the system is more loose with the orbital period $P_{orb} \sim 1year$ and with circular orbit. The companion is a low mass helium white dwarf with mass $M \leq 0.4M_{\odot}$. At present six double neutron stars are known.

Observations of double neutron stars are very important. Shrinking of the orbit in the pulsar PSR 1913+16 is the best indication available of gravitational radiation. Also, precise determination of masses of both neutron stars is possible for double neutron stars. This is crucial for constraining models of neutron star interior.

Binary radio pulsars play also important role in our understanding of the evolution of neutron stars in binaries, as is discussed below.

2.4. Thermally radiating single neutron stars

Astrophysicists expect that there are some $\sim 10^8$ neutron stars in our Galaxy. These are remnants of previous generations of massive stars which produced all the metals (i.e. $Z > 2$ elements) observed at present. Many of these stars should be hot enough and close enough to be observable as X-ray sources. Recently, the first such star was observed both in X-ray band [7] and in UV and visible band by the Hubble Space Telescope [2]. The neutron star is hot and it was first observed as a strong X-ray source by the ROSAT satellite. The star emits thermal radiation and is located about 130 pc from Earth. This allows for the first time to directly constrain the radius of a neutron star to be $R \leq 14km$ [2].

2.4.1. Invisible neutron stars

Nonrotating and nonaccreting neutron stars which have cooled down are virtually undetectable by conventional means. Such stars contribute to the dark matter of the Galaxy

in the form of massive compact objects. Recently, gravitational microlensing experiments have detected a population of such objects in the galactic halo [8]. Future microlensing observations are crucial for determination of the contribution of invisible massive baryonic objects to the total mass of the Galaxy. In particular they should answer the question if there is a halo of neutron stars around our Galaxy. Such a halo composed of stars which obtained sufficiently high initial velocity at birth would explain scarcity of local thermally radiating neutron stars.

2.5. Physical parameters of neutron stars

Observations of neutron stars in all astrophysical objects discussed above allow us to determine some of their physical parameters. The relevant parameters are the mass, the radius, the temperature, the age and the magnetic field. Generally, simultaneous measurement of all above parameters for a given neutron star is not possible.

2.5.1. Neutron star masses

Presently, masses of about 20 neutron stars in binary systems are determined. Among them are six double neutron star binaries, PSR B1913+16 [9], PSR B1534+12 [10], PSR B2303+46 [11], PSR B2127+11C [12], PSR B1820-11 [13] and PSR J1518+4904 [14]. For three of them, PSR B1913+16, PSR B1534+12 and PSR B2127+11C, precise measurements of mass of both neutron stars are now available. The masses are found to be $M_1 = 1.44M_\odot$ and $M_2 = 1.39M_\odot$ (PSR B1913+16), $M_1 = 1.34M_\odot$ and $M_2 = 1.34M_\odot$ (PSR B1534+12) and $M_1 = 1.35M_\odot$ and $M_2 = 1.36M_\odot$ (PSR B2127+11C). All masses lie in a rather narrow interval, $1.3M_\odot < M < 1.5M_\odot$. Masses of neutron stars in X-ray pulsars are also consistent with these values although are measured less accurately. The measured masses of neutron stars apparently do not exceed the maximum mass which is about $1.5M_\odot$. We shall discuss possible implications of this upper limit in the last section.

2.5.2. Neutron star radii

The first observation of thermally radiating nonpulsating neutron star RX J185635-3754 [2,7] constrains the radius of the star to be $R < 14km$. Generally, radii of neutron stars are not directly observable. One can infer, however, some plausible values from model calculations of X-ray bursters which are of the order of $10km$.

2.5.3. Surface temperature of neutron stars

The X-ray and optical spectrum of the neutron star RX J185635-3754 corresponds to the black body with $k_B T \approx 60 eV$. Also, the X-ray flux from about 14 pulsars has been detected [15]. The spectrum of photons is more difficult to obtain. If measured, it is often not consistent with the thermal emission but is rather dominated by a hard component due to the magnetospheric activity. Only for four pulsars, PSR 0833-45 (Vela), PSR 0630+18 (Geminga), PSR 0656+14 and PSR 1055-52, softer blackbody component corresponding to surface thermal emission is determined.

2.5.4. The age of pulsars

Pulsar ages are estimated by measuring their spin-down rates. Pulsars spin down due to conversion of rotational energy into radiation. A simple spin-down relation is assumed, $\dot{\nu} = K\nu^n$, where ν is the rotation frequency, and n is the braking index. The constant K for magnetic braking is proportional to d^2/I , where d is the magnetic moment of the star and I is the moment of inertia. If the energy loss is through radiation from a dipolar magnetic field, the braking index is $n = 3$. The spin-down age of pulsar is then $\tau = -\nu/2\dot{\nu}$.

The spin-down age with $n = 3$ is commonly used for pulsars. Its applicability, however, is questioned by recent measurement of the braking index of the Vela pulsar [16], which gives $n = 1.4 \pm 0.2$. This value implies that previous estimate of the age of Vela pulsar should increase by a factor ~ 3 .

Typical values of the spin-down age for radio pulsars are $10^7 y$. For millisecond pulsars the spin-down age exceeds $10^9 y$.

2.5.5. Magnetic fields of neutron stars

Magnetic fields of radio pulsars are inferred from the spin-down relation assuming dipolar magnetic field. A striking feature is the bimodal distribution of pulsar magnetic fields. Usual pulsars have strong magnetic field, $B \sim 10^{11} - 10^{13} G$, whereas millisecond pulsars possess much weaker fields, $B \sim 10^8 - 10^{10} G$. For some X-ray pulsars the magnetic field is measured directly, by observation of absorption features interpreted as cyclotron lines [17]. The values are in the range found for normal pulsars. It should be noted that neutron stars in the X-ray bursters have, if any, weaker fields, $B < 10^{10} G$.

The magnetic field of neutron stars could also serve as a probe of the neutron star equation of state (EOS) if its presence is determined by the properties of dense matter. The bimodal distribution of pulsar magnetic fields strongly suggests existence of a magnetic

phase transition in the neutron star matter [17]. There is a possibility, however, that some component of the magnetic field of a neutron star is inherited from the progenitor.

The magnetic phase transition in the neutron star matter is discussed in Sect.4.

3. FORMATION OF NEUTRON STARS

Neutron stars are the final product of stellar evolution. The evolution of single stars is significantly different than the evolution of stars in binaries. The formation scenario of neutron stars in binary systems reflects this fact. We briefly discuss below both cases.

3.1. Evolution of single stars

Life of single stars with the mass $M \geq 8M_{\odot}$ is terminated by the supernova explosion. The explosion is a result of the gravitational collapse of the star's iron core whose mass has exceeded the Chandrasekhar mass, $M_{Ch} \approx 1.5M_{\odot}$, the maximum mass which can be supported by pressure of the electron gas. The collapse is halted when the density increases sufficiently for the nucleons to feel the repulsive core of their mutual interaction. The nuclear interactions produce very steep pressure gradient which is able to stop the collapse. Rapid release of the gravitational energy, which is carried mostly by neutrinos, causes the violent explosion of outer layers of the star. The total amount of the energy released in the gravitational collapse of the stellar core is $\sim 10^{53}erg$. Only $\sim 1\%$ of this energy is needed to expel the mantle and envelope of the collapsing star. The basic scenario of the Type II supernova explosion was spectacularly confirmed by detection by the Kamiokande experiment of the neutrino burst associated with the supernova SN 1987A. The energy of neutrinos and the distance to the Large Magellanic Cloud, where SN 1987A occurred, allows to estimate the total energy carried by neutrinos to be $\sim 10^{53}erg$.

3.2. Evolution of binaries

Evolution of stars in close binaries in which stars can exchange mass proceeds differently than for single stars. Evolution of binaries relevant to neutron star formation depends on the initial mass and separation of the primary and secondary star. Below we discuss the origin of high mass X-ray binaries and low mass X-ray binaries and their evolutionary links to binary and millisecond pulsars.

3.2.1. Formation of high mass X-ray binaries

The progenitor of the high mass X-ray binary is a binary system with the primary star heavier than the O or B star present in such X-ray binaries, $M_1 > M_2$. This star evolves

quickly and explodes as a supernova. In general, the binary system can be disrupted by the supernova explosion. However, if the mass ejected from the system is less than the mass left,

$$M_{ejected} < M_2 + M_{NS} \quad (2)$$

where M_{NS} is the mass of the neutron star, the binary binding can survive [18]. Also, a suitable natal kick imparted to the neutron star at birth in asymmetric supernova explosion, can save the binary from disruption. For the produced system to become an X-ray binary sufficient accretion onto the neutron star is required. Since the newly formed neutron star has a strong magnetic field, it becomes an X-ray pulsar when it accretes matter from the normal companion. Such an interacting binary system can be formed for a range of masses and orbital separations of the primary and secondary stars of the progenitor.

3.2.2. Origin of double neutron stars

There exist scenarios linking the formation of the binary pulsars of PSR 1913+16 class to the evolution of high mass X-ray binaries. In these models the evolution proceeds through the common envelope phase. The companion of the neutron star in the high mass X-ray binary, which is primary as far as the mass is concerned, evolves quite fast. When it approaches the red giant phase, its expanding hydrogen envelope can engulf the neutron star. The binary system enters a hypothetical period of common envelope evolution. The neutron star is expected to spiral inward due to friction, getting closer to the helium core. In this process, the envelope which is weakly bound is thought to become expelled. As a result, a binary system of the neutron star and the helium star, is formed. The mass of the helium star is about $3M_{\odot}$. Such a helium star after some time undergoes core collapse and explodes as a supernova which leaves a remnant neutron star. Detailed considerations suggest [19] that only in an asymmetric supernova explosion a binary system of two neutron stars can be formed.

The binary pulsar PSR 1913+16, which is a double neutron star, has likely followed such an evolutionary track. Similar evolutionary considerations are valid for other pairs of neutron stars. These systems are observed as binary radio pulsars with a neutron star companion. An important question is which of the two neutron stars is the radio pulsar. The fact, that the pulsar in PSR 1913+16 has period $59ms$ and low magnetic field $B \sim 2 \times 10^{10}G$ suggests that it is a recycled pulsar with the age $\sim 10^8y$. Newly formed neutron star is expected to have much stronger magnetic field, $B \sim 10^{12}G$, and to live as

a radio pulsar only $\sim 10^7$ years. Hence it is more likely that we observe as a radio pulsar the older neutron star in this binary.

The orbits of binary pulsars with neutron star companions shrink due to gravitational radiation. The two neutron stars will collide/merge in some $10^9 y$. The collision/merger is unavoidable. In such a violent event a lot of energy will be liberated in a rather short time interval and the collision can manifest itself as a powerful explosion. Many researchers consider such a neutron star collision the best candidate for gamma-ray bursters.

3.2.3. Formation of low-mass X-ray binaries

The origin of low mass X-ray binaries is more difficult to explain [20]. Most of evolutionary models base on common envelope evolution prior to the supernova explosion. The major problem is the asymmetry of masses of assumed progenitors of these binaries. The masses of donor stars, which are companions of neutron stars, are low, $M \leq 1.2M_{\odot}$, and these stars are unevolved. The mass of the primary of the progenitor must be high enough in order to produce a neutron star. It can exceed the secondary mass, which is the donor mass of low mass X-ray binary by a factor ≥ 20 . The evolutionary sequence leading to the low mass X-ray binary consists of several steps. First, a common envelope forms, due to small time scale of nuclear evolution of the massive primary. During this phase the hydrogen envelope is dispersed and the binary orbit is shrunk. Otherwise, if the primary explodes as a supernova before the envelope is expelled the system becomes disrupted. After the common envelope phase the binary system with a helium star emerges. The chance the system survives the explosion of the helium star is increased, in particular the asymmetric explosion imparting a proper kick to the neutron star can help.

An alternative scenario of formation of low mass X-ray binaries is the accretion-induced collapse of the white dwarf. In this model, the Chandrasekhar mass white dwarf collapses to the neutron star when some matter is accreted onto it. The progenitor binary consists of two low mass stars, with the heavier one becoming the carbon white dwarf. It remains an open question if the accretion induced collapse of the white dwarf occurs in nature. One should remember that the carbon white dwarf contains a lot of nuclear fuel which can undergo thermonuclear flash, that completely disrupts the star. Such an explosive carbon burning of a white dwarf in a binary is a successful model of the Type I supernovae. No remnant star is left in such an explosion.

Those binaries which sustain low accretion rates for a very long time are observed as low mass X-ray binaries. Magnetic fields of neutron stars in these binaries seem to be

low, $B \leq 10^{10}G$. One popular explanation is that the magnetic field, initially of the order $10^{12}G$ has decayed due to accretion.

3.2.4. Origin of millisecond pulsars

Accretion in low mass X-ray binaries lasts for such a long time that a total mass of a few tenths of solar mass, $M_{tot} \sim 0.1M_{\odot}$, is transferred from the low mass star to the neutron star. When the accretion ceases the donor is thus a helium white dwarf typically with $M \leq 0.4M_{\odot}$. The neutron star which has accreted $\sim 0.1M_{\odot}$ is spinning rapidly due to acquiring additional angular momentum transferred by the accreted matter. The magnetic field of the neutron star is now weaker but the neutron star can manifest itself as the millisecond pulsar in the binary system. The neutron star becomes a recycled pulsar. Thus low mass X-ray binaries seem to be progenitors of binary millisecond pulsars [21].

There are several examples of binary millisecond pulsars with very low mass companion. The pulsar PSR 1744-24A with $P = 11.6ms$ has the companion of mass $M_c = 0.1M_{\odot}$ and the $1.61ms$ pulsar PSR 1957+20 has the one with $M_c = 0.02M_{\odot}$. Apparently, millisecond pulsars in these binaries evaporate their companion stars. The binding energy of low mass stars is $E_b \leq 10^{48}(M_c/M_{\odot})^2 erg$ whereas the rotational energy of the pulsar is $E_{rot} = I\omega^2/2 \sim 10^{52}P_{ms}^{-2}erg$. The pulsar can evaporate the companion if $E_b \leq gE_{rot}$, where the factor g is the efficiency of evaporation. Complete evaporation of the low mass companion by the millisecond pulsar is currently the preferred scenario of the formation of single millisecond pulsars [22].

4. STRUCTURE OF NEUTRON STARS

The internal structure of neutron stars is determined by properties of matter at super-nuclear densities which are subject to considerable uncertainty. At densities close to the saturation density the composition of neutron star matter can be determined unambiguously by simple extrapolation from laboratory data. With increasing density, one needs to employ models of nucleon interactions which introduce some uncertainty. The higher the density the less reliable is the equation of state. In particular, composition of dense matter can change and new degrees of freedom, such as hyperons, condensed meson fields and quarks should be taken into account.

There exist recent reviews of physics of neutron star matter [23] and the equation of state [24]. I have selected some topics relevant to internal properties of neutron stars in the density range where most likely the neutron star matter is composed of nucleons

and leptons only. I will focus on possible localization of protons and spin ordering in the neutron star matter. Existence of such a phase can influence magnetic fields of neutron stars.

4.1. Crust

We shall focus on structure of physically relevant neutron star of mass $\sim 1.4M_\odot$. The surface of the star is defined at the radius where pressure vanishes. Just below the surface the pressure is dominated by the degenerate electrons of the solid crust. The crust is similar to matter from which white dwarfs are made of. It is the lattice of bare nuclei immersed in the electron sea. With increasing density, deeper in the star, a layer occurs where the mean matter density becomes equal to the nuclear matter density $n_0 = 0.17fm^{-3}$. This is the boundary of the neutron star core. The core is composed of nucleon liquid of densities exceeding the saturation density, $n > n_0$.

4.2. Neutron star core

The material, from which the neutron star core is built of, is condensed hadronic matter, essentially in the ground state. Such matter is named cold catalysed matter. Just below the crust, the core matter is composed mainly of neutrons with some admixture of protons, electrons and muons. This matter is condensed since the Fermi energy of electrons is much higher than the thermal energy, $E_F \gg k_B T$. Thermal energy of particles in the neutron star is below $1MeV$, except of first few minutes after formation. The temperature of a newly born neutron star is $k_B T \sim 10MeV$. The star cools to $k_B T \sim 1MeV$ in a few minutes. The electron Fermi energy in the core is $E_F \sim 100MeV$.

Weak interactions ensure that the neutron star matter relaxes to β -equilibrium with neutron, proton and electron chemical potentials satisfying the condition

$$\mu_N = \mu_P + \mu_e. \quad (3)$$

When the electron chemical potential exceeds the muon rest mass, $\mu_e \geq m_\mu = 106MeV$, muons appear in the matter with the chemical potential $\mu_\mu = \mu_e$.

The neutron star matter is locally charge neutral, with the lepton (electrons + muons) density equal to the proton density,

$$n_e + n_\mu = n_P. \quad (4)$$

4.2.1. Neutron star matter at density n_0

Properties of neutron star matter of saturation density can be inferred from empirical parameters of nuclear matter which are obtained from nuclear mass formulae. The empirical value of nuclear symmetry energy, $E_s = 31 \pm 4 \text{ MeV}$ allows one to fix the proton fraction by using Eq.(3) and (4). The proton fraction, $x = n_P/n$, of β -stable nucleon matter of saturation density is $x(n_0) \approx 0.05$.

The surface layer of the neutron star core, of density $n_0 \approx 0.17 \text{ fm}^{-3}$, is the only part of the core whose composition is determined quasi-empirically. The value of the proton fraction, $\sim 5\%$, is known with accuracy determined entirely by the empirical error of the nuclear symmetry energy.

The composition of β -stable matter of density n_0 is found by minimization of the energy of charge neutral nucleon matter with leptonic contribution with respect to proton fraction. The energy per baryon is

$$E(x) = E_{nuc}(x) + E_{lepton}(x), \quad (5)$$

where the nucleon contribution is

$$E_{nuc}(x) = E_0 + E_s(2x - 1)^2. \quad (6)$$

In the last formula $E_0 = -16 \text{ MeV}$ is the saturation energy of symmetric nuclear matter. The formula (6) is the $A \rightarrow \infty$ limit of the semiempirical mass formula.

The lepton contribution consists of both electron and muon parts, $E_{lepton} = E_e + E_\mu$. Muons appear in the system when the electron chemical potential exceeds the muon rest mass, $\mu_e \geq 106 \text{ MeV}$, which happens at $n_e \geq 0.005 \text{ fm}^{-3}$. The lepton part can be calculated exactly. At densities where $n_\mu = 0$, the electron part is $E_e = 250(n_B/n_0)^{1/3}x^{4/3} \text{ MeV}$, and in the high density limit with $n_e = n_\mu$, $E_{lepton} \rightarrow 200(n_B/n_0)^{1/3}x^{4/3} \text{ MeV}$.

The minimum of $E(x)$ occurs at $x \approx 0.05$. Hence the macroscopic nuclear matter of density n_0 consists of protons, neutrons, electrons and muons with densities $n_P = 0.05n_0$, $n_N = 0.95n_0$, $n_e = 0.99n_P$ and $n_\mu = 0.01n_P$. At the minimum the electron chemical potential is $\mu_e = \mu_\mu = \mu_N - \mu_P = 110 \text{ MeV}$. The energy per baryon is $E = 8 \text{ MeV}$. The properties of neutron star matter of density n_0 are fully determined by the empirical parameters of nuclear matter.

4.2.2. Neutron star matter at higher densities

For densities $n > n_0$ no direct empirical data relevant to the neutron star matter are available. In order to study its properties one must resort to models of nucleon matter. There exist a variety of realistic models of nucleon matter. One class is based on effective interactions, such as Skyrme forces [25] or Myers and Swiatecki interactions [26]. These are generally developed by fitting properties of finite nuclei. Another class is based on phenomenological potentials, such as e.g. Reid soft core potential [27], Urbana v_{14} potential [28] or Argonne v_{14} potential [29], and employs variational many-body theory to calculate the equation of state of dense matter [30]. Phenomenological potentials are constrained to fit the nucleon-nucleon scattering and the properties of the deuteron. The models provide energy per particle as a function of proton and neutron density. This allows us to calculate chemical potentials of protons and neutrons and to construct the EOS of β -stable neutron star matter.

Despite the fact that the realistic models predict rather different equations of state, there is one qualitative feature which is similar: the proton fraction of the β -stable neutron star matter, $x(n_B)$ (Fig.2). Generally, realistic models predict that the proton fraction is low, $x(n) \leq 0.1$, and, as a function of baryon density n_B , decreases with n_B . At high enough densities protons eventually disappear from β -stable neutron star matter. The density n_v at which the proton fraction vanishes is model dependent. From Fig.2 one can see that $n_v \sim 0.5 fm^{-3}$ for some parametrization of Skyrme forces and $n_v \approx 1.0 fm^{-3}$ for the UV14+TNI interactions. For Myers and Swiatecki interactions $x(n_B)$ drops slowly with density.

Generally, realistic models of nucleon matter lead to a qualitative prediction that at high densities proton content of neutron star matter decreases and eventually vanishes. At densities slightly lower than n_v protons are impurities in the neutron star matter. In the following we shall discuss properties of such a strongly asymmetric nuclear matter which have important consequences for neutron stars.

4.2.3. Why do protons disappear?

It seems strange at first sight that at densities $n_B > n_v$ pure neutron matter is β -stable. This behaviour can be understood as a result of nucleon-nucleon interactions used in realistic models of the nucleon matter.

The fact that proton fraction vanishes at density n_v means that the minimum of the energy per baryon (5) occurs at this density for the first time at $x = 0$. This can be traced

back to the behaviour of the nucleon contribution, E_{nuc} [31]. In analogy with Eq.(6) we write the nucleon energy in the form

$$E_{nuc}(n_B, x) = E_{nuc}(n_B, \frac{1}{2}) + E_s(n_B)(2x - 1)^2, \quad (7)$$

where $E_{nuc}(n_B, \frac{1}{2})$ is the energy of symmetric nuclear matter at density n_B and $E_s(n_B)$ is the symmetry energy at n_B . As long as the symmetry energy is positive, $E_s(n_B) > 0$, the minimum of the total energy $E_{nuc} + E_{lepton}$ occurs at some finite proton fraction $x \neq 0$. However, when $E_s = 0$, the minimum occurs at $x = 0$. This means that the density n_v corresponds to vanishing of the symmetry energy, $E_s(n_v) = 0$. At higher densities, $n_B > n_v$, the symmetry energy is negative, $E_s(n_B) < 0$.

Change of sign of the symmetry energy is the immediate cause of disappearance of protons. With $E_s < 0$, Eq.(5) shows the energy per particle of pure neutron matter ($x = 0$) is lower than for any $x > 0$. It is thus energetically favourable for the system to get rid of all protons and negatively charged leptons [32].

4.2.4. Microscopic origin of proton disappearance

The β -stability condition (3) at the density n_v becomes

$$\mu_N(n_v, x = 0) - \mu_P(n_v, x = 0) = 0 \quad (8)$$

as the electron chemical potential also vanishes. The formula (8) allows us to understand the microscopic origin of the phenomenon of proton disappearance.

The chemical potential of neutrons is the neutron Fermi energy which has both kinetic and interaction contributions,

$$\mu_N = E_{kin}(k_N^F) + E_{int}^{NN}, \quad (9)$$

where k_N^F is the neutron Fermi momentum and E_{int}^{NN} is the interaction energy of the neutron at the Fermi surface with other neutrons. The proton chemical is

$$\mu_P = E_{int}^{PN}, \quad (10)$$

where E_{int}^{PN} is the interaction energy of zero momentum proton with surrounding neutrons. Formally, this is the Fermi energy of an empty proton Fermi sea and the proton Fermi momentum is $k_P^F = 0$.

From Eq.(8) we see that

$$E_{int}^{PN} > E_{int}^{NN}. \quad (11)$$

The fact the proton-neutron interaction energy is higher than neutron-neutron interaction energy means that in the underlying nucleon-nucleon potentials the proton-neutron repulsion is stronger than the neutron-neutron one. For several phenomenological potentials this really is the case. The central potentials for the proton-neutron channel and the neutron-neutron one can be written as $v_{PN} = v_c - v_\tau$ and $v_{NN} = v_c + v_\tau$ where v_c and v_τ are central and isospin components of general nucleon-nucleon potential

$$v_{nucleon-nucleon}(r) = v_c(r) + v_\tau \vec{\tau}_1 \vec{\tau}_2 + \dots \quad (12)$$

where dots represent not displayed contributions (tensor, spin, spin-orbit, etc.). The v_τ component for popular potentials is shown in Fig.3. As one can see, $v_\tau < 0$, and thus $v_{PN} > v_{NN}$.

4.3. Proton impurity in the neutron star matter

Nuclear matter in neutron stars which contains only small admixture of proton impurities displays some new features, not encountered at higher proton concentrations. Below we show that impurities likely become localized at high densities. This means that nucleon matter is no longer a simple Fermi liquid. Particularly important for neutron stars is the ferromagnetic instability of neutron matter with localized protons.

The first observation is that the proton impurity couples to density fluctuations [33] of the neutron matter with the interaction Hamiltonian of the deformation-potential form. To show this let us consider the energy of a single proton in the uniform neutron matter of density n_N , which can be written in the form [34]

$$E_P(\vec{k}) = \frac{k^2}{2m_*} + \mu_P(n_N). \quad (13)$$

The single impurity case corresponds to $\vec{k} \rightarrow 0$. The last term in this formula represents the interaction energy of the proton impurity with the neutron matter. As shown above, this is the proton chemical potential.

Let us assume that there are small density oscillations in the neutron matter,

$$n(\vec{r}, t) = n_N + \delta n(\vec{r}, t). \quad (14)$$

The Hamiltonian of the proton impurity in the presence of small density oscillations becomes

$$H_P = -\frac{\nabla^2}{2m_*} + \mu_P(n_N) + \frac{\partial\mu_P}{\partial n_N}\delta n(\vec{r}, t). \quad (15)$$

The last term represents the coupling of the proton impurity to phonons of the neutron matter. After quantizing the oscillations we obtain [33] the deformation-potential coupling of Bardeen and Shockley [35] for the polaron problem in solids. This interaction is characterized by the deformation-potential coupling constant

$$\sigma = \frac{\partial\mu_P}{\partial n_N}n_N. \quad (16)$$

The coupling vanishes for the density where the proton chemical potential in pure neutron matter has the minimum [33]. This density is close to n_0 . At higher densities σ increases with density [33].

The proton impurity induces a virtual hole in the neutron medium which moves with it. The hole can be interpreted as a phonon cloud accompanying the proton. The proton impurity displays thus a typical polaron behaviour [33]. This affects the effective mass of the impurity which is now the nuclear polaron mass, $m_{\text{polaron}} > m_*$.

The regime of small values of the deformation-potential coupling σ corresponds to so called large polaron [33]. With increasing σ one enters the strong coupling regime where eventually the polaron becomes localized [33]. The localized polaron is also called small polaron. Localization of the proton impurity, which is the nuclear polaron, corresponds to freezing of the deformation of the neutron background. This is a phase transition. The localization is a selfconsistent trapping of the proton wave function in the potential well corresponding to the hole induced by the impurity in the neutron background. The localization density n_{loc} depends on the model of nucleon interactions. In Ref.[33] we have found $n_{loc} \sim 3n_0$ for the UV14+TNI interactions.

4.4. Ferromagnetic instability of neutron star matter with localized protons

It is easy to see that a single localized proton induces a spin excess of the neutron background provided any proton-neutron spin interaction exists. The nucleon-nucleon interactions are of course strongly spin dependent and thus there always exists some proton-neutron spin interaction,

$$v_{spin} = v_{\sigma}(r)\vec{\sigma}_N\vec{\sigma}_P. \quad (17)$$

Since this spin interaction is linear the proton spin can always be arranged in such a way that the net effect is attractive. For a fixed neutron spin, if $v_{\sigma} > 0$ ($v_{\sigma} < 0$) the proton spin should be antiparallel (parallel) with respect to the neutron spin. For a single proton, there is no Pauli blocking and the proton spin can be changed with no increase of the kinetic energy. It is thus obvious that the system will relax to the spin ordered configuration with the lowest energy [34]. Such a configuration will possess induced spin excess of the neutron background in the vicinity of the proton impurity [34].

At low proton fractions, the above analysis also applies [36]. The neutron star matter which contains localized protons exhibits ferromagnetic instability [37]. One can identify mechanism by which the long-range order is produced [38]. This is the well known RKKY mechanism operating e.g. in rare-earth alloys. The basic physics is as follows. The spin excess of the neutron background induced by a given proton extends outside the region where the proton wave function is localized. In this way a neighbouring localized proton is polarized in the direction of the spin of the first proton, etc. A long-range ferromagnetic order can propagate in the system.

4.4.1. Neutron stars with ferromagnetic core

Neutron star matter with localized protons is magnetized [36]. The magnetization can be parametrized as [40]

$$M = \mu_{eff}n_P, \quad (18)$$

where μ_{eff} is the effective magnetic moment of the localized proton [36]. Typical values of magnetization are $M \sim 10^{13}G$ [39]. This value is rather similar to typical magnetic fields of normal radio pulsars.

The contribution of the magnetized neutron star matter to pulsar magnetic field was considered in [40]. If the proton localization density is less than the central density of the neutron star, $n_{loc} < n_c$, the star develops the ferromagnetic core. Such a core produces a magnetic moment of the neutron star.

4.5. Empirical constraints on the equation of state of neutron star matter

Current theoretical models do not predict the internal structure of neutron stars and their equation of state in a unique way. With increasing density a wide range of possibilities

occurs as far as relevant degrees of freedom are concerned. Uncertainties regarding the equation of state and the internal structure are discussed in Ref.[41].

The EOS of neutron star matter at high densities is not at present constrained sufficiently by theory to allow conclusive statements as to the internal structure of neutron stars. In view of weakness of theoretical constraints it is urgent to empirically constrain the EOS.

4.5.1. Laboratory experiments

Scattering of heavy ions, which is the only laboratory way to study properties of dense matter, does not probe directly the EOS relevant to neutron stars. In nuclear collisions highly excited hadronic matter is formed which decays quickly into stable particles. One should perform extrapolations in order to obtain the ground state properties of β -stable matter from these data which would involve considerable uncertainty. However, many important informations regarding the neutron star EOS can be inferred from scattering data. In particular, interactions of hyperons formed in nuclear collisions with nucleons in dense fireball can be studied. Also, detection of quark-gluon plasma in heavy ion collisions could give valuable informations about energy density range in which one can expect deconfinement transition in neutron star matter.

4.5.2. Observations of neutron stars

Discovery of a sub-millisecond pulsar would severely constrain the EOS. Unfortunately, reported observations of 0.5 ms pulsar in the SN1987A remnant [42] turned out to be erroneous. The fastest millisecond pulsar of period 1.56 ms does not exclude any realistic EOS.

4.5.3. X-rays from rotation-powered pulsars

Observations of thermal flux of photons from a pulsar, whose age can be estimated, can provide information how fast the neutron star cools. Probing the cooling curve of neutron stars is considered to be the most profitable method to learn about the internal composition of neutron stars.

Recent observations of thermal X-ray flux from four pulsars give promise that in near future the cooling curve will be empirically constrained. The main objective of these observations is to discriminate between fast and slow cooling mechanisms.

Slow cooling proceeds mainly through the modified URCA process,

$$n + n \rightarrow n + p + e^- + \bar{\nu}_e, \quad n + p + e^- \rightarrow n + n + \nu_e.$$

It is the dominating mechanism of standard cooling scenario for neutron stars whose proton content is below the critical value, $x < x_{URCA} \approx 0.11$.

If the proton content exceeds the critical value, $x > x_{URCA}$, or there exists kaon (or pion) condensate in the neutron star matter, cooling proceeds through direct URCA process,

$$n \rightarrow p + e^- + \bar{\nu}_e, \quad p + e^- \rightarrow n + \nu_e.$$

This cooling mechanism is much faster, and, correspondingly, the temperature of the neutron star is lower than for modified URCA.

Recent comparison of the X-ray luminosities of four pulsars [43] is not conclusive, but the observational data are somewhat closer to the standard cooling curve.

4.5.4. Remnant of SN1987A

Detection of the neutrino flux associated with optical observations of the supernova SN1987A was the best confirmation of the theory of neutron star formation in supernova Type II explosions. Present observations of the light curve of the remnant of SN1987A do not confirm existence of the neutron star. Continuously decreasing luminosity of the remnant of SN1987A suggests that Crab-like pulsar does not exist in the remnant. Also, no hot X-ray source is observed. This lack of signature of the neutron star has led some authors [44] to speculate that the neutron star formed initially in SN1987A was in a metastable state and subsequently collapsed to a black hole. Presence of the black hole in SN1987A would strongly constrain the neutron star EOS.

Scenario of black hole formation in SN1987A is as follows. The progenitor star of SN1987A is known to have mass $18M_\odot < M < 20M_\odot$. Evolutionary calculations show that this star developed an iron core of mass $\sim 1.6M_\odot$ which collapsed to form hot neutron star. This neutron star existed at least for $\sim 10s$, a period when the neutrino emission took place. After radiating away the trapped neutrinos the neutron star has lost stability and collapsed to black hole.

This scenario requires that the EOS has some unique features. The maximum mass corresponding to the hot neutron star matter, with trapped neutrinos, M_{max}^{hot} , has to be higher than the mass $M_{ns} \sim 1.6M_\odot$ of the neutron star formed in the collapse of SN1987A,

$M_{ns} < M_{max}^{hot}$. After emitting neutrinos the neutron star loses stability which requires that its mass is higher than the maximum mass of a neutron star corresponding to cold neutron star matter, $M_{max}^{cold} < M_{ns}$. The EOS with kaon condensation can meet these constraints [45]. The maximum mass for cold EOS is $M_{max}^{cold} = 1.5M_{\odot}$.

The maximum mass of neutron star of $1.5M_{\odot}$ explains in a natural way the cutoff observed in measured masses of neutron stars. Existence of such a limit is very surprising in view of the fact that considerable amount of material, at least a few tenths of solar mass, is expected to fall back onto newly formed neutron star after the explosion. One would expect many heavier neutron stars to be formed.

If the maximum mass of neutron star is $M_{max} = 1.5M_{\odot}$ then one can determine maximum mass of the progenitor star, whose collapse can leave the neutron star remnant. For an isolated star this mass is about $20M_{\odot}$. Heavier stars are expected to leave black hole remnants.

This work is partially supported by the Polish State Committee for Scientific Research (KBN), grants 2 P03D 001 09 and 2 P03B 083 08. The author is grateful for inviting him to give these lectures at the XXV Mazurian Lakes School of Physics.

References

1. S. L. Shapiro and S. A. Teukolsky, *Black Holes, White Dwarfs and Neutron Stars*, Wiley, 1983.
2. F. M. Walter and L. D. Matthews, *Nature* **389**, 358 (1997).
3. F. Camilo, S. E. Thorsett, and S. R. Kulkarni, *Astrophys. J.* **421**, L15 (1994).
4. F. Haberl, L. Angelini, C. Motch, and N. E. White, astro-ph/9710138.
5. L. Bildsten et al., astro-ph/9707125.
6. R. A. Hulse and J. H. Taylor, *Astrophys. J.* **195**, L51 (1975).
7. F. M. Walter, S. J. Wolk, and R. Neuhäuser, *Nature* **379**, 233 (1996).
8. C. Alcock et al., *Astrophys. J.* **445**, 133 (1995).
9. J. H. Taylor and J. M. Weisberg, *Astrophys. J.* **345**, 434 (1989).
10. A. Wolszczan, *Nature* **350**, 688 (1991).
11. S. E. Thorsett, Z. Arzoumanian, M. M. McKinnon and J. H. Taylor, *Astrophys. J.* **405**, L29 (1993).

12. W. T. S. Deich and S. R. Kulkarni, in *Compact Stars in Binaries*, eds J. van Paradijs, E. P. J. van den Heuvel and E. Kuulkers eds., Dordrecht, Kluwer 1996.
13. Z. Arzoumanian, Ph. D. thesis, Princeton Univ. (1995).
14. D. J. Nice, R. W. Sayer and J. H. Taylor, *Astrophys. J.* **466**, L87 (1996).
15. H. Ögelman, in *The Lives of Neutron Stars*, eds M. A. Alpar, U. Kiziloglu and J. van Paradijs eds., Dordrecht, Kluwer 1995.
16. A. G. Lyne, R. S. Pritchard, F. Graham-Smith and F. Camilo, *Nature* **381**, 497 (1996).
17. K. Makishima, in *The Structure and Evolution of Neutron Stars*, eds D. Pines, R. Tamagaki and S. Tsuruta, Addison-Wesley 1992.
18. A. Blaauw, *Bull. Astron. Inst. Neth.* **505**, 265 (1961).
19. C. Fryer and V. Kalogera, astro-ph/9706031.
20. V. Kalogera and R. F. Webbink, astro-ph/9708223.
21. E.P.J. van den Heuvel, in *Neutron Stars: Theory and Observation*, eds J. Ventura and D. Pines, Kluwer 1991.
22. M. Tavani, in *Neutron Stars: Theory and Observation*, eds J. Ventura and D. Pines, Kluwer 1991.
23. G. Baym, in *Neutron Stars: Theory and Observation*, eds J. Ventura and D. Pines, Kluwer 1991.
24. J. M. Lattimer, in *The Structure and Evolution of Neutron Stars*, eds D. Pines, R. Tamagaki and S. Tsuruta, Addison-Wesley 1992.
25. D. Vautherin and D. M. Brink, *Phys. Lett.* **32B**, 149 (1970).
26. W. D. Myers and W. J. Swiatecki, *Nucl. Phys. A* **601**, 141 (1996).
27. R. V. Reid, *Ann. Phys.* **50**, 411 (1968).
28. I. E. Lagaris and V. R. Pandharipande, *Nucl. Phys.* **A359**, 331, 349 (1981).
29. R. W. Wiringa, R. A. Smith and T. L. Ainsworth, *Phys. Rev. C* **29**, 1207 (1984).
30. R. W. Wiringa, V. Fiks and A. Fabrocini, *Phys. Rev. C* **38**, 1010 (1988).
31. M. Kutschera, *Z. Phys. A* **348**, 263 (1994).
32. M. Kutschera, *Phys. Lett.* **B340**, 1 (1994).
33. M. Kutschera and W. Wójcik, *Phys. Rev. C* **47**, 1077 (1993).
34. M. Kutschera and W. Wójcik, *Acta Phys. Pol.* **B21**, 823 (1990).
35. J. Bardeen and W. Shockley, *Phys. Rev.* **80**, 72 (1950).
36. M. Kutschera and W. Wójcik, *Phys. Lett.* **B223**, 1 (1989).

37. M. Kutschera and W. Wójcik, Nucl. Phys. **A581**, 706 (1994).
38. M. Kutschera and W. Wójcik, Acta Phys. Pol. **A92**, 375 (1997).
39. M. Kutschera and W. Wójcik, Acta Phys. Pol. **B27**, 2227 (1996).
40. M. Kutschera and W. Wójcik, Acta Phys. Pol. **B23**, 947 (1992).
41. M. Kutschera, in *Solar Astrophysics, Structure of Neutron Stars, Gamma Flares*, ed. K. Grotowski, Polish Academy of Arts and Sciences, Cracow, 1997.
42. C. Kristian, et al., Nature **338**, 234 (1989).
43. Ch. Schaab, F. Weber, M. K. Weigel and N. K. Glendenning, astro-ph/9603142.
44. G. E. Brown, S. W. Bruenn and J. C. Wheeler, Comments Astrophys. **16**, 153 (1992).
45. V. Thorsson, M. Prakash and J. M. Lattimer, Nucl. Phys. **A572**, 693 (1994).

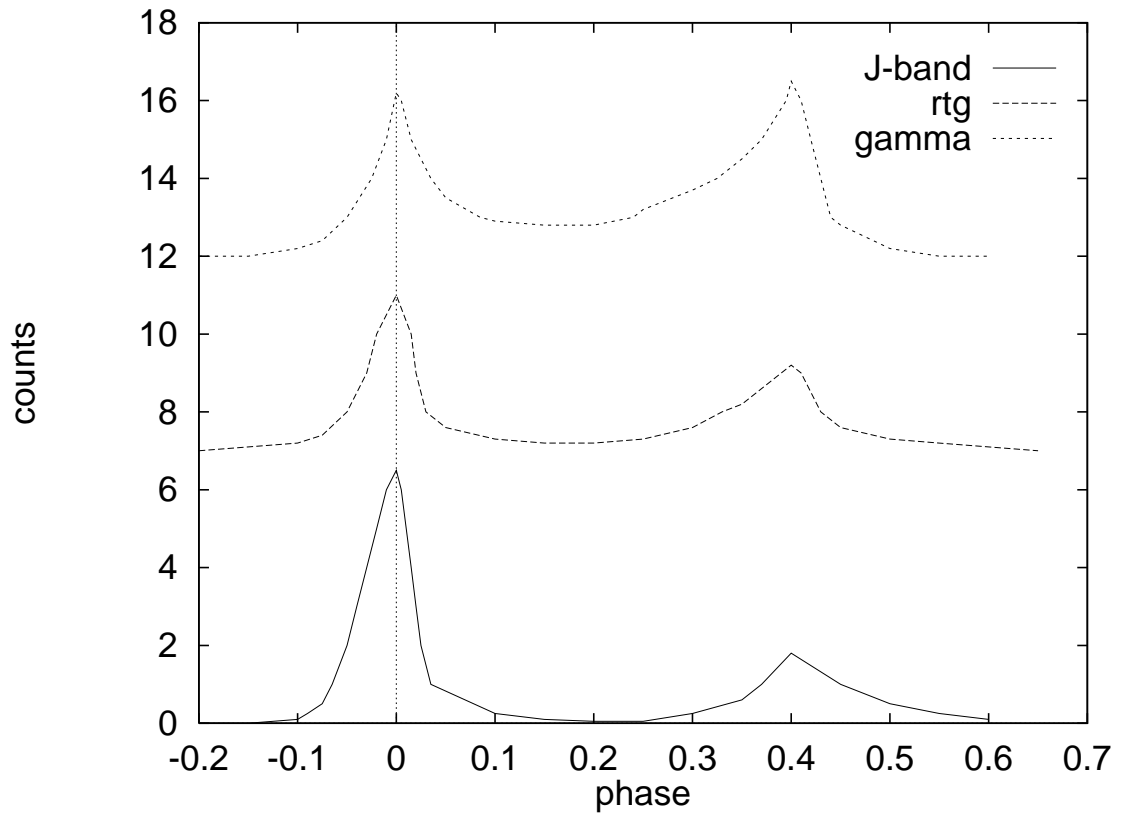


Fig.1

The pulse profile of the Crab pulsar in infrared J-band, X-rays and γ -rays. Curves for different bands are shifted vertically. Units on vertical axis are arbitrary.

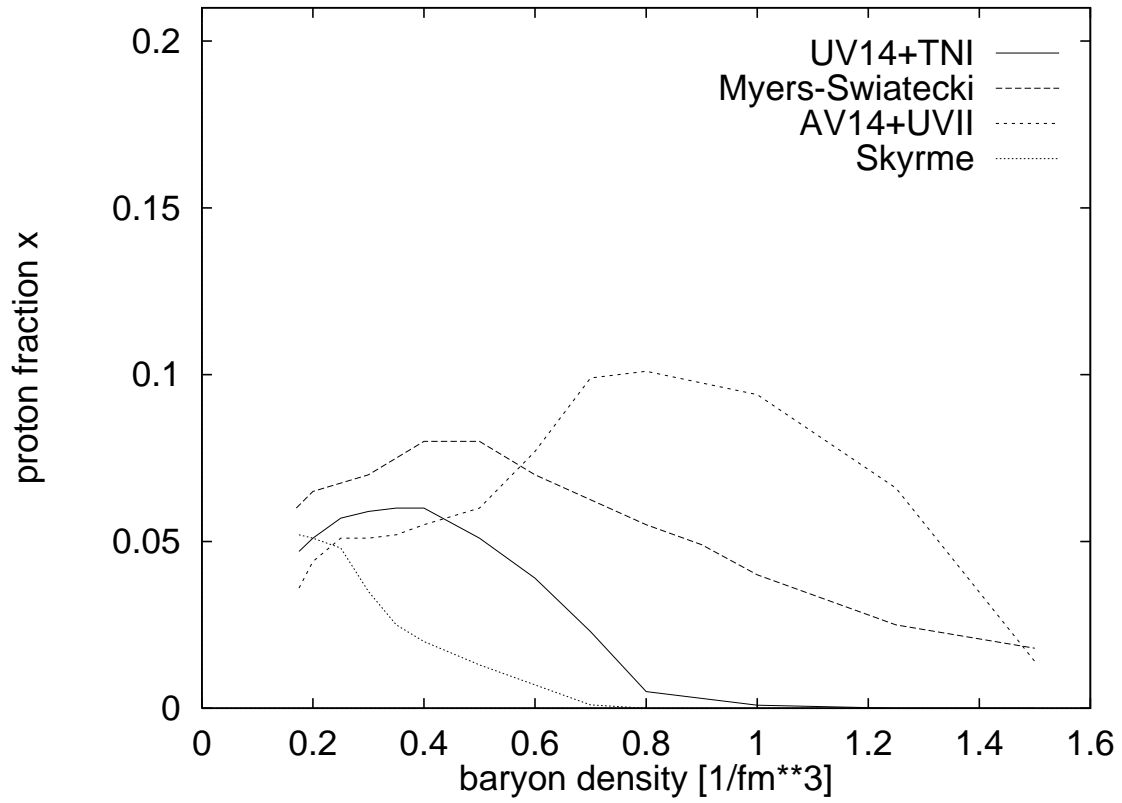


Fig.2

The proton fraction x as a function of density for realistic models of neutron star matter based on Skyrme forces, Myers and Swiatecki interactions, and on Urbana v_{14} and Argonne v_{14} potentials.

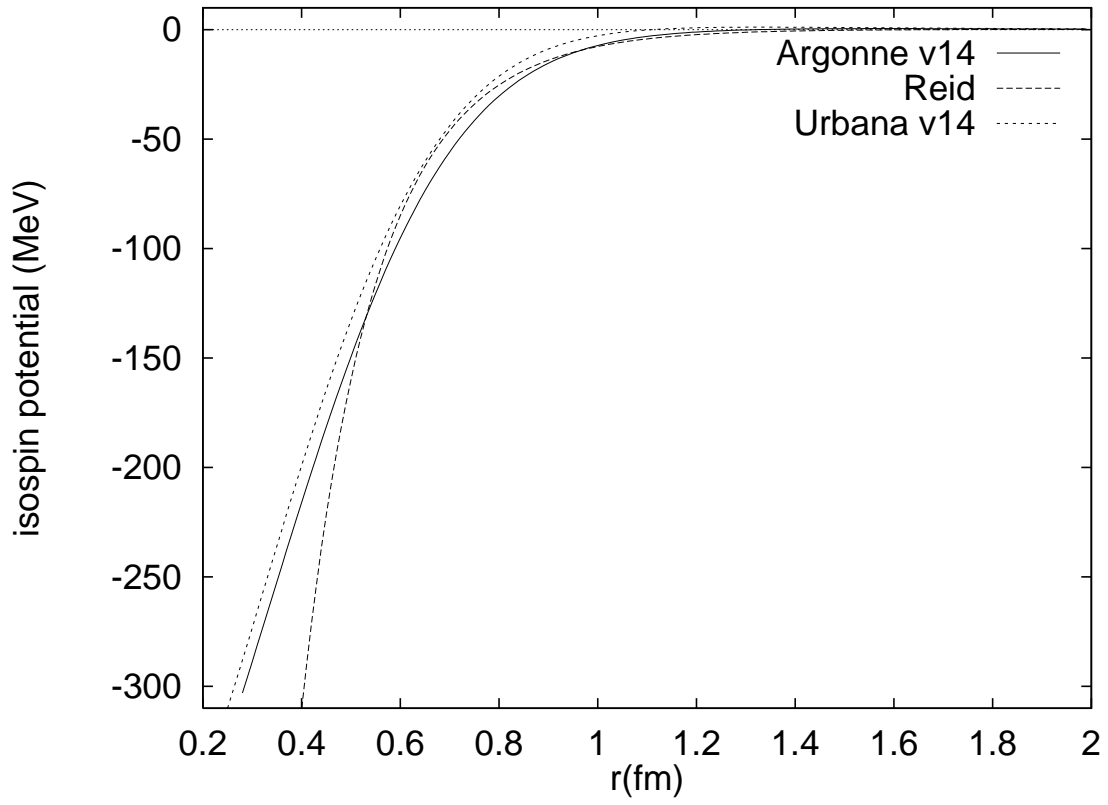


Fig.3

The isospin potential v_τ of Reid, Argonne v_{14} , and Urbana v_{14} nuclear potentials.